

[HP99] 159 – Properties of the first Supersoft X-ray Source with a Helium star donor

Hélène Szegedi¹*, Philip A. Charles^{1,2,3}, David A. H. Buckley^{1,4,5}, Pieter J. Meintjes¹, Przemek Mróz⁶, and Andrzej Udalski⁶

¹Department of Physics, University of the Free State, 205 Nelson Mandela Drive, Bloemfontein, 9300, RSA

²Department of Physics and Astronomy, University of Southampton, Southampton, Hampshire, SO17 1BJ, United Kingdom

³Astrophysics, Department of Physics, University of Oxford, Keble Road, Oxford OX1 3RH, UK

⁴South African Astronomical Observatory, PO Box 9, Observatory Road, Observatory 7935, South Africa

⁵Department of Astronomy, University of Cape Town, Private Bag X3, Rondebosch 7701, South Africa

⁶Astronomical Observatory, University of Warsaw, Al. Ujazdowskie 4, 00-478 Warsaw, Poland

Accepted XXX. Received YYY; in original form ZZZ

ABSTRACT

[HP99] 159 is remarkable as the first supersoft X-ray source (SSS) identified with an evolved helium star donor. With a likely orbital period of 1.164 d or 2.327 d, the origin of the SSS component is controversial, with the two current models being either steady He-burning on the white dwarf surface, or that it is a helium nova in the decaying phase. To help resolve this issue we present extensive new long-term spectroscopy (with SALT) and photometry (at SAAO and with OGLE) of [HP99] 159 which (a) supports 2.327 d as the orbital period, and (b) finds only a small He II radial velocity modulation. The latter is surprising as it implies a very low inclination system, whereas our light curve modelling suggests $i \sim 50^\circ$, and hence that the He II must be produced in outflowing material further above, or beyond, the disc. We find that the decaying nova model cannot fit our OGLE light curve and the observed SSS flux level. [HP99] 159 has been essentially constant as an SSS over several decades, implying a sustained high level of mass-transfer from its He star donor, making it the only confirmed single-degenerate scenario SN Ia progenitor. We have updated the known SSS binary parameters and find a clear ~ 1.5 mag difference in their M_V when compared to the $M_V - \Sigma$ properties of LMXBs, likely due to the larger irradiated areas and more luminous donors.

Key words: X-rays: individual([HP99]159) – white dwarfs – binaries: close – supernovae: general

1 INTRODUCTION

In spite of being detected in X-ray surveys over the last ~ 30 years, [HP99] 159 was only recently recognised as a new LMC X-ray source by Greiner et al. (2023). Based on its very soft X-ray spectrum (blackbody $kT \sim 40\text{--}45$ eV, with a radius of ~ 3700 km) and relatively high luminosity ($L_X \sim 7 \times 10^{36}$ erg s $^{-1}$), they suggested that it was a new member of the SSS (“supersoft” X-ray sources) class (Kahabka & van den Heuvel 2006), where the emission arises from “steady” thermonuclear burning of material on the surface of a white dwarf (WD). What made [HP99] 159 remarkable, though, was that its optical counterpart showed no hydrogen lines in its spectrum, only helium, leading Greiner et al. (2023) (hereafter, G23) to identify it as the first SSS to be driven by accretion from a helium star. Such a system is potentially of great interest in the study of supernova type Ia progenitors, as one of the evolutionary routes is the SD (single-degenerate) channel in which a WD is accreting at very high rates (see Ruiter 2020, and references therein) from a highly evolved donor. Furthermore, G23’s analysis of archival data on [HP99] 159 from ROSAT through to XMM and eROSITA indicated that its X-ray emission and spectrum appeared remarkably stable throughout.

From their inferred WD radius, G23 calculated its mass to be $M_1 = 1.20^{+0.18}_{-0.40} M_\odot$ and that it was accreting material via an accretion disc fed by a helium star. Their long-term photometry revealed modulations at 1.1635 days, and its weak harmonic at 2.327 days, which were identified as possible orbital periods, and high resolution spectra appear to indicate a low inclination angle binary.

The source of the supersoft X-ray component, however, has been challenged by Kato et al. (2023), who point out that steady He burning on the WD surface requires an $\dot{M}_{\text{acc}} \sim 10^{-6} M_\odot \text{ yr}^{-1}$, which is much higher (by almost a factor 10) than that inferred by G23’s observed L_X . While G23 argue that stable burning at lower accretion rates is possible for rapidly rotating WDs (Yoon & Langer 2004; Wong & Schwab 2019), Kato et al. (2023) offer a very different explanation. They suggest that [HP99] 159 is a helium nova similar to V445 Pup (e.g. Kato & Hachisu 2003; Woudt & Steeghs 2005) that erupted ~ 28 years ago, and is currently being observed during the decay phase.

We therefore undertook an observational campaign to look for evidence of [HP99] 159 being a possible decaying helium nova, to confirm the absence of hydrogen in the system, and to constrain P_{orb} through extensive phase-resolved spectroscopy, as well as further photometry.

* E-mail: SzegediH@ufs.ac.za

Table 1. SALT/HRS spectroscopic observing log of [HP99] 159

Date	HJD (Start) (2450000+)	Resolution Mode	$n_{\text{data}} \times t_{\text{exp}}$ (s)
2022-12-26, 27, 30, 31	9940-9945	Low	1 \times 2400
2023-01-01	9946	Low	1 \times 2400
2023-01-12, 13, 14	9957-9959	Low	1 \times 2400
2023-01-30, 31	9975-9976	Low	1 \times 2400
2023-02-09	9985	Low	1 \times 2400
2023-02-12, 13	9988-9989	Low	1 \times 2400
2023-03-02	10006	Low	1 \times 2400
2023-03-12	10016	Low	1 \times 2400
2023-03-17	10021	Low	1 \times 2400
2023-11-17	10266	Medium	2 \times 1800
2024-01-31	10341	Low	1 \times 2500
2024-02-05, 08, 09	10346-10350	Low	1 \times 2500

Note: The number of data frames is n_{data} and the exposure time per frame is t_{exp} .

2 OBSERVATIONS AND DATA REDUCTIONS

Optical spectroscopic and photometric observations of [HP99] 159 were conducted between December 2022 and October 2024 at the Sutherland station of the South African Astronomical Observatory (SAAO). The photometric data was supplemented with OGLE-IV data.

2.1 Spectroscopy

2.1.1 SALT/HRS

High resolution spectroscopy was performed with the 11-m Southern African Large Telescope (SALT; [Buckley et al. 2006](#)) equipped with a dual-beam fiber-fed echelle high resolution spectrograph (HRS; [Bramall et al. 2010, 2012; Crause et al. 2014](#)). The observations were conducted under program 2021-2-LSP-001 (PI: David Buckley) on 21 epochs between December 2022 and February 2024. The HRS covers the spectral range of 3740–8780 Å (blue camera $\lambda = 3740\text{--}5560$ Å, red camera $\lambda = 5450\text{--}8780$ Å). It has three resolution modes, namely low ($R = 14000\text{--}15000$), medium ($R=40000\text{--}43000$) and high ($R=67000\text{--}74000$). Our observations were carried out in low and medium resolution modes, with Table 1 providing more details.

The primary HRS data reduction was performed with the SALT pipeline PySALT ([Crawford et al. 2010](#)), which included bias subtraction, cross-talk correction, plus gain and overscan correction. The MIDAS HRS automatic pipeline¹ ([Kniazev et al. 2016, 2017](#)) was used to perform the spectroscopic reductions which included flat-field corrections, order extraction, wavelength calibration with arc spectra of ThAr+Ar lamps, sky subtraction, and 2D to 1D spectral extraction.

2.1.2 1.9-m telescope and SpUpNIC

[HP99] 159 was observed on 3 October 2024 with the SAAO 1.9-m telescope equipped with the SpUpNIC Cassegrain spectrograph ([Crause et al. 2016](#)) using grating 4, giving a resolution of 1.8 Å with the 1.5 arcsec slit width. A CuAr lamp provided wavelength

¹ <https://astronomers.salt.ac.za/software/hrs-pipeline/>

Table 2. SAAO 1.0-m/SHOC photometric observing log of [HP99] 159

Date	HJD (2460000+)	$t_{\text{exp}} \times n_{\text{data}}$ (s)
2024-01-03	313	20 \times 426
2024-01-04	314	15 \times 987
2024-01-05	315	15 \times 818
2024-01-06	316	15 \times 726
2024-01-08	318	15 \times 200
2024-01-17	327	15 \times 726
2024-01-18	328	15 \times 522
2024-01-19	329	15 \times 726
2024-01-20	330	15 \times 420
2024-01-21	331	15 \times 576
2024-01-22	332	15 \times 242
2024-01-23	333	15 \times 484
2024-01-24	334	15 \times 726
2024-01-29	339	30 \times 81

Note: The exposure time per frame is t_{exp} , and n_{data} is the number of data frames.

calibration. Three science frames were obtained with an exposure time of 1200 sec for each.

Standard IRAF routines ([Massey 1997](#)) were used to perform bias and flat field correction, and the spectra were wavelength-calibrated using the CuAr arc frames. Flux calibration was performed with respect to the spectrophotometric standard star, LTT 7987, observed on the same night. The spectra were co-added to obtain one average spectrum.

2.2 Photometry

The SAAO 1.0-m telescope equipped with SHOC, the Sutherland High-speed Optical Camera² ([Coppejans et al. 2013](#)) was utilized for photometry of [HP99] 159. The observations were performed in conventional mode i.e. utilizing a 1 MHz 16-bit conventional amplifier, with a pre-amp gain of 2.5 and 2x2 binning. No filters were used, meaning that [HP99] 159 was observed in “white light”. The details of these observations are summarized in Table 2.

TEA-PHOT³, a Python-based pipeline developed by [Bowman & Holdsworth \(2019\)](#) specifically for SHOC data cubes, was exploited to perform our data reductions. Although capable of producing differential light curves from CCD reductions and adaptive elliptical aperture photometry, we only used it to slice the data cubes, obtaining the correct time stamps per frame (including the Barycentric Julian Date in the Dynamical Time standard at mid-exposure), and to perform bias subtraction and flat-field correction.

[HP99] 159 is located in the LMC, a crowded stellar field, and so we used the DAOPHOT package in IRAF to perform PSF (Point-Spread Function) photometry. A weighted differential photometry procedure was applied, following the same method as discussed by [Everett & Howell \(2001\)](#) and [Burdanov et al. \(2014\)](#). Two comparison stars of similar brightness to the target, and which had the lowest mean variance were utilized.

² Further details on SHOC can be obtained from <https://www.saaو.ac.za/science/facilities/instruments/shoc/>.

³ <https://bitbucket.org/DominicBowman/tea-phot/>

2.3 OGLE-IV photometric data

The Optical Gravitational Lensing Experiment (OGLE) is a long-term, large-scale photometric survey focused on sky variability, including detecting microlensing events, and has been operational from the early 1990s (Udalski et al. 1992). It regularly monitors hundreds of millions of stars in the Galactic Bulge, Galactic Disc, and Magellanic Cloud regions and, hence, monitored [HP99] 159 during the fourth phase of the project (OGLE-IV). See Udalski et al. (2015) for a detailed description of the observing setup and data calibration. Here, we analyze OGLE-IV observations collected between 2010 and 2024. The data for [HP99] 159 were obtained in the I -band filter with typical exposure times of 150 s. The photometry was performed using the difference image analysis technique (Alard & Lupton 1998) as implemented by Wozniak (2000). The DIA pipeline implemented by OGLE returns underestimated photometric errors, so we applied the formula $\sigma_{\text{new}} = \sqrt{(\gamma \times \sigma_{\text{old}})^2 + \epsilon^2}$ (where $\gamma = 1.058$, $\epsilon = 0.0051$ for the OGLE field containing [HP99] 159) specified by Mróz et al. (2024) to correct the OGLE-IV magnitude errors. Note that this represents a statistical error and does not fully capture the intrinsic uncertainty associated with the scatter.

3 RESULTS

3.1 Photometric variability

The 14-year OGLE-IV I -band light curve (Figure 1) shows that [HP99] 159 remained within ± 0.1 mag of $I \sim 16$ throughout this interval. A linear model fitted to the data indicated a slope of -0.0007 ± 0.0006 mag yr $^{-1}$ (brightness increase) and a horizontal shift of 15.9897 ± 0.0027 mag. A t-test indicated that the null hypothesis slope of zero at a 3σ confidence level (99.73%) cannot be rejected. This provides evidence that the system has not declined over time.

We also compared the OGLE-IV light curve with the decaying nova model (and a slow X-ray decay of $\tau_{\text{SSS}} = 120$ yr) proposed by Kato et al. (2023). The X-ray light curve of the decaying nova model was converted to M_V using the correlation $M_V = 0.83 - 3.46 \log \Sigma$, where $\Sigma = (L_X/L_{\text{Edd}})^{1/2} (P/1\text{hr})^{2/3}$, derived by van Teeseling et al. (1997) for SSS. Since the X-ray light curve only accounts for the SSS contribution, a He star flux was added so that the total system brightness scaled to fit through the OGLE-IV data at the time of the XMM-Newton and eRosita observations. The total contribution M_V was converted to V -mag and a $V - I = 0.06$ offset (obtained from G23 Extended Data Fig. 3) was added. The model is plotted in Figure 1 using two age options for the nova outburst: 28 yr ago (blue line) and 80 yr ago (purple line).

In the OGLE interval, the 28 yr decay model has an almost linear slope of $+0.00351 \pm 0.00001$ mag yr $^{-1}$ (brightness decrease) and a t-test rejects a null hypothesis slope of zero at a 3σ confidence level (99.73%). The 80 yr decay model has a much shallower linear slope of $+0.000974 \pm 0.000001$ mag yr $^{-1}$ (brightness decrease) and a t-test indicates a null hypothesis slope of zero (3σ confidence level; 99.73%) cannot be rejected. While the 80 yr decay model is consistent with the OGLE data, we reject it since the model fits very poorly to the observed SSS fluxes, as also noted by Kato et al. (2023). These results, together with the fact that the blackbody temperature has also been stable for the past 30 years, does not support the decaying helium nova scenario, as even the most shallow decline consistent with the observations in their Fig. 3 would have been detectable in the OGLE data.

As in G23, we performed a Lomb-Scargle (LS) analysis of the

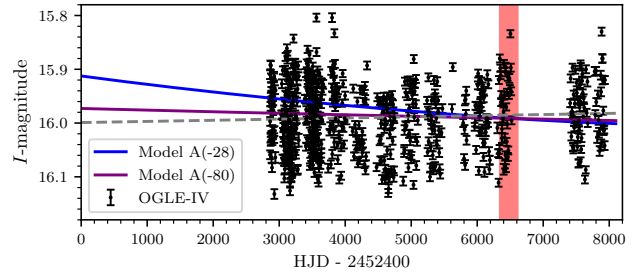


Figure 1. OGLE-IV I -band light curve of [HP99] 159 obtained Mar 2010 – Jan 2024, with a linear fit (dashed line) giving a mean of $I=16$, and demonstrating no detectable decline over the last 14 yrs. The blue and purple lines represent the 28 yr and 80 yr decaying nova models, respectively, of Kato et al. (2023). The red region indicates the time interval of the XMM-Newton and eROSITA observations.

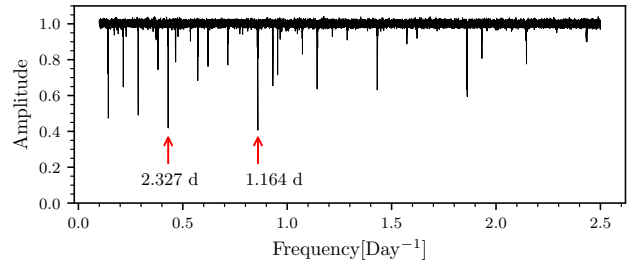


Figure 2. PDM periodogram of the OGLE-IV light curve (Fig. 1) in the frequency range of $0.1 < f < 2.5$ cycles day $^{-1}$. The two strongest signals are marked, and are the same as those seen in our and G23's Lomb-Scargle periodograms.

OGLE-IV light curve, and also strongly detected modulations at $P = 1.1635 \pm 0.0001$ d and a weaker signal at $P = 2.3269 \pm 0.0003$ d (our periodogram is essentially identical to G23's Fig. 4a). Since G23 favoured the 2.3 d signal as a possible orbital period (due to its lower variance), we decided to perform a phase dispersion minimization (PDM) period analysis, as it is insensitive to the light curve shape, and is able to determine periods with high accuracy. We used the *pdm* task in the Starlink PERIOD package (Version 5.0-2), selecting 20 bins (each of width 0.11 d) and a frequency range of $0.1 < f < 2.5$ cycles day $^{-1}$. The resulting PDM is shown in Figure 2 and clearly detected both modulations, with them now being of essentially equal strength.

The light curve of [HP99] 159 obtained with the SAAO 1.0-m/SHOC (3 – 29 Jan 2024) was phase-folded on the suggested P_{orb} of 2.327 d (Figure 3), using BJD2455255.443 as T_0 . It displays the same double-humped light curves typically seen in accreting close binary systems, and is in agreement with that of G23. We therefore also support a P_{orb} of 2.327 d.

3.2 Spectroscopic variability

The 1.9-m/SpUpNIC spectrum (Figure 4), covering the wavelength range $\lambda \sim 3820 - 5050$ Å, is very similar to that of G23 Fig. 2. In particular, this purely emission-line spectrum shows no hydrogen (Balmer) lines, only those attributable to He I and He II.

The high resolution spectra obtained with SALT/HRS also support the results of G23, as seen in the detailed He II and He I line profiles of Figure 5. They are all double-peaked He emission lines, evidence of an established accretion disc, together with changes in

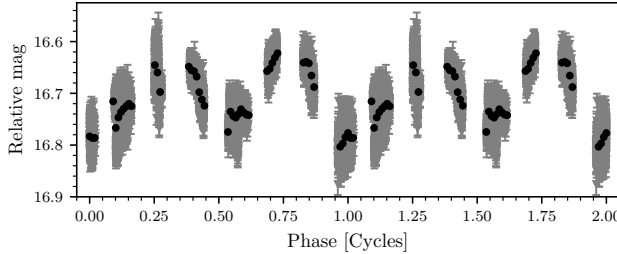


Figure 3. The phase-folded light curve on the proposed 2.33 d orbital period obtained with the SAAO 1.0-m/SHOC (3 – 29 Jan 2024). Two cycles are shown for clarity.

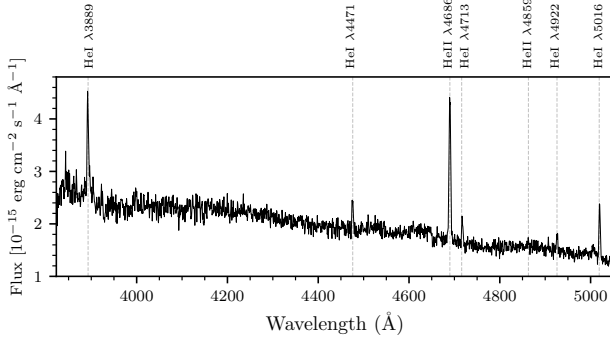


Figure 4. SAAO 1.9-m/SpUpNIC spectrum of [HP99] 159 on 3 Oct 2024. All the emission lines are attributed to He I and He II, confirming the absence of hydrogen.

the asymmetry of the profiles that is typical, and often attributed to the hot spot (created by the mass-transfer stream impacting the disc) rotating with the orbital period. A peak separation of $\sim 100 \text{ km s}^{-1}$ implies an outer disc velocity of $\sim 50 \text{ km s}^{-1}$ and the wings of the emission lines indicate an inner disc velocity of $\sim 150 \text{ km s}^{-1}$. These values are low for accretion discs in close interacting binaries, indicating that the system is likely being viewed from a very low inclination angle if the lines arise only from the disk modulated by the Keplerian and orbital motions.

3.3 Radial velocity curves

With our extensive SALT spectroscopy of [HP99] 159 (Table 1) we could study the radial velocity (RV) curves of these emission lines. To measure K , we applied the method of Shafter (1983). The wings of the two strongest emission lines, He II $\lambda 4686$ and He I $\lambda 7065$, were fitted with Gaussian functions to determine their central wavelengths. The resulting barycentric-corrected RV curves of He II and He I are plotted in the middle and bottom panels of Figure 6, respectively, along with the OGLE-IV light curve (top panel), all phase-folded on $P_{\text{orb}} = 2.327$ d. A sine function was fitted to the He II RV curve (red dashed line), giving a systemic velocity of $\gamma = 273 \pm 1 \text{ km s}^{-1}$ and a semi-amplitude of the accretion disc of $K_{\text{disc}} = 9 \pm 1 \text{ km s}^{-1}$. The He I RV data points clearly show no significant modulation, but interestingly do show a mean RV offset of $\sim 10 \text{ km s}^{-1}$ with respect to He II. The lack of RV modulation for He I indicates that the He II emission is originating from a region close to the WD, while the He I likely comes from further out in the accretion disc, where the velocities are lower.

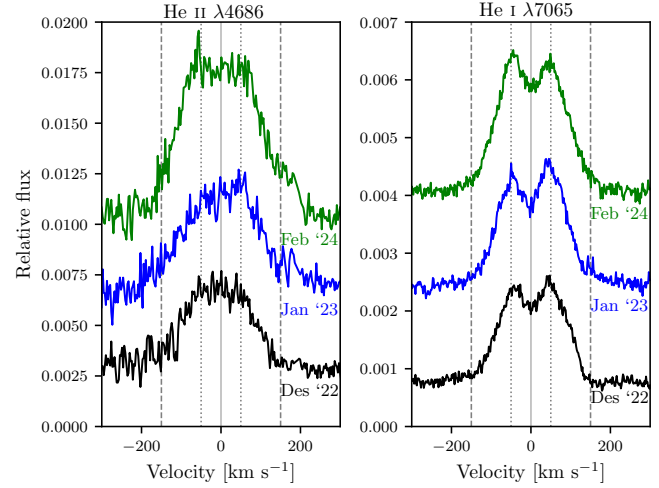


Figure 5. He II and He I line profiles in SALT/HRS spectra, obtained between Dec 2022 and Feb 2024. The plots are offset vertically by an arbitrary constant.

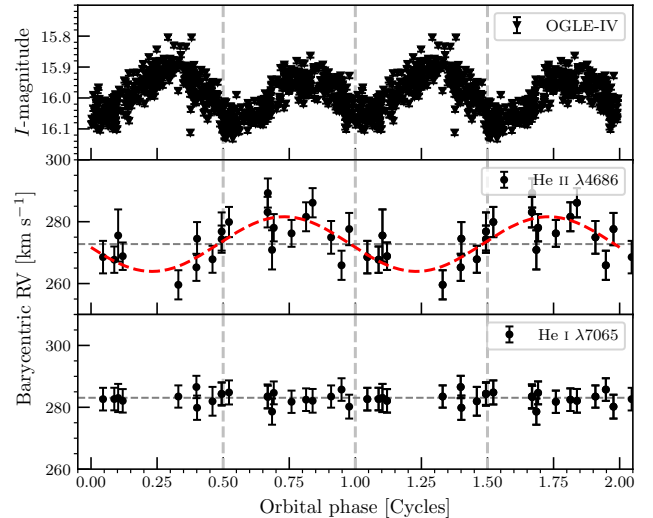


Figure 6. *Top panel:* The phase folded OGLE-IV light curve. *Middle panel:* He II $\lambda 4686$ radial velocity curve. A sine fit (red dashed line) gives $K_1 \sim 9 \pm 1 \text{ km s}^{-1}$. *Bottom panel:* He I $\lambda 7065$ radial velocity curve. Two cycles are shown for clarity. Error bars show $\pm 1\sigma$.

Assuming a circular orbit and the white dwarf located at the centre of an axisymmetric accretion disc, then the K_1 value for the WD (assumed = K_{disc}) together with $P_{\text{orb}} = 2.327$ d gives us the donor's mass function

$$\frac{M_2^3}{(M_1 + M_2)^2} \sin^3 i = \frac{P_{\text{orb}}}{2\pi G} K_1^3 \quad (1)$$

i.e. $f(M_2) = 1.75 \times 10^{-4} M_{\odot}$ and is clearly indicative of a low-inclination system ($i < 5^\circ$ for $M_2 \geq 1 M_{\odot}$). Furthermore, from P_{orb} we know from Kepler's 3rd Law that the size of the binary must be $a = 7.4(M_1 + M_2)^{1/3} R_{\odot}$.

Table 3. Estimated binary parameters of [HP99] 159 for three donor masses

Parameter	$M_2 = 0.8 M_\odot$	$M_2 \geq 1.2 M_\odot$	$M_2 = 2 M_\odot$
$M_1 (M_\odot)$	1.2	1.2	1.2
$q (= M_2/M_1)$	0.67	≥ 1	1.7
$R_1 (R_\odot)$	3.9	< 3.8	3.7
$R_2 (R_\odot)$	3.2	> 3.8	4.6
i (degrees)	6.4	< 4.8	3.5

4 DISCUSSION

4.1 Binary parameters

While the WD mass was constrained by G23 to be $M_1 = 1.20^{+0.18}_{-0.40} M_\odot$ based on the measured X-ray blackbody radius, the absence of hydrogen in the disc led them to assume that it must be accreting from a He star, which must be filling its Roche-lobe in order to drive the necessarily large mass transfer rates. This implies a He star donor with mass in the range $M_2 \sim 0.8 - 2.0 M_\odot$ (see also Kato et al. 2023 who derive similar masses). For unstable mass transfer proceeding on a thermal timescale, thereby driving a high accretion rate (Kahabka & van den Heuvel 2006) means that the mass ratio $q (= M_2/M_1) \geq 1$ for the inferred massive WD. However, to reproduce the low RV semi-amplitude, such masses also imply a very low orbital inclination, namely $i \sim 3.5 - 4.8$ degrees.

Given that the He star must be filling its Roche-lobe, we can use the Eggleton (1983) approximation to:

$$\frac{R_2}{a} = \frac{0.49q^{2/3}}{0.6q^{2/3} + \ln(1 + q^{1/3})} \quad \text{for } 0 < q < \infty, \quad (2)$$

to estimate the He star radius (and by replacing q with q^{-1} , we can also calculate the WD's Roche lobe radius, R_1). This yields the binary parameters given in Table 3.

Helium stars with these properties have been modelled by Götberg et al. (2018), with their Fig. 2 (see also Kato et al. 2023, Fig. 4) indicating that a $\sim 4 M_\odot$ star will enter the mass transfer phase when it has expanded to sizes comparable to that calculated in Table 3. We also chose such relatively low mass He stars based on the optical model spectra presented in their Fig. 5. More massive stars ($> 7 M_\odot$) can be excluded, as they would exhibit much more powerful, broader He II emission lines that are typical of Wolf-Rayet stars. The much narrower, weaker emission features seen in our spectra are almost certainly driven by the SSS component, and not the donor. Indeed, the model He star spectra of Götberg et al. (2018) in the lower mass range show only weak Balmer absorption features, and even they would be undetectable as a result of the mass-transfer stripping of the hydrogen envelope, leaving the bare He star to build up a helium-dominated accretion disc that feeds the WD.

4.2 Can we believe the low inclination?

There are a number of reasons why we should treat such a low inferred i value from the radial velocity curve with caution, although there are important caveats.

(i) on statistical grounds, pole-on binaries are rare. It is well-known (based on solid angles on the sky) that a random distribution of orbital axis orientations has a chance of i values that is proportional to $\sin i$;

(ii) however, there may also be observational selection effects at work. One of these is the ease with which the very low energy SSS

X-rays can be absorbed by intervening matter, and this is particularly true at higher binary inclinations where the mass transfer stream and disc material itself can block the SSS component. This means they are more readily detectable when observed at lower inclinations;

(iii) such a low i is not consistent with our observed photometric modulation (Figure 6 top panel). [HP99] 159 could be considered as a contact binary, and the simulated light curves of Rucinski (2001) imply that $i \sim 40^\circ$ is needed to produce an ~ 0.1 mag amplitude modulation;

(iv) the prototypical SSS RXJ0513.9-6951 has a similar He II emission line RV curve (Southwell et al. 1996) with a low K_1 of 14.5 km s^{-1} that would infer $i < 7^\circ$, yet it also displays weaker satellite emission lines displaced by $\pm 3900 \text{ km s}^{-1}$ from the main feature. These are interpreted as jets emitted perpendicular to the plane of the disc, travelling with at least the WD escape velocity, again arguing against a low inclination, as also indicated by its photometric light curve;

(v) our double-peaked He I line profile in Figure 5 is a classic feature of accretion discs in CVs and LMXBs, and is taken as arising from advancing and receding material towards the outer disc. Again, this would not be expected in a very low-inclination system.

4.3 Light curve modelling

Since the simulated light curves of Rucinski (2001) suggest that we should be considering higher inclination values, we decided to investigate this in more detail by using PHOEBE (Version 2.4.21; Prša et al. 2016) to model the OGLE-IV light curve of [HP99] 159. PHOEBE is a software package that is used for eclipsing binaries, but does not include accretion physics. However, given that the “steady” SSS requires ongoing high levels of mass transfer into the accretion disc around the WD (as depicted in Hachisu & Kato 2003, Fig.3) we have approximated this as an A0 star orbiting the He star, and used PHOEBE to build synthetic light curves at different i . We note a similar approach was used in Smak et al. (2001) in modelling the double-humped light curve of V Sge, a high mass transfer cataclysmic variable. The accretion discs in such systems are bloated and cannot be modelled as standard accretion discs (see e.g. Hachisu & Kato 2003).

The simulated system was treated as a contact binary with the stars in circular orbit. The binary parameters $P_{\text{orb}} = 2.327 \text{ d}$, $a = 10.9 R_\odot$ and $q = 1.67$ were fixed and we assumed an A0 star ($M_1 = 1.2 M_\odot$, $T_{\text{eff}} = 10000 \text{ K}$) to represent the WD+hot disc. An effective temperature of $T_{\text{eff}} = 15850 \text{ K}$ was set for a $M_2 = 2 M_\odot$ He star. The stellar radii were set to the respective Roche lobe radii ($R_1 = 3.66 R_\odot$ and $R_2 = 4.6 R_\odot$).

The OGLE-IV light curve was converted to flux (using the Vega flux zeropoint⁴, Czesla et al. 2019) and normalized, and plotted with the synthetic light curves at different i in Figure 7. A χ^2 analysis indicates that the synthetic light curve with $i = 50^\circ$ fits the OGLE-IV data the best with a reduced $\chi^2 = 6.4$ (Figure 7 insert). As PHOEBE does not model accretion discs and hot spots, it cannot model the excess emission above the synthetic light curve at phase 0.25 contributed by the hot spot in [HP99] 159.

This does leave us with conflicting indications for i , but based on the unlikelihood of pole-on systems we believe the higher i implied by the light curves to be more likely. We then assume that the He II must be produced in outflowing material further above, or lost from, the disc and hence will display a diluted RV modulation. This is

⁴ <https://github.com/szczesla/PyAstronomy>

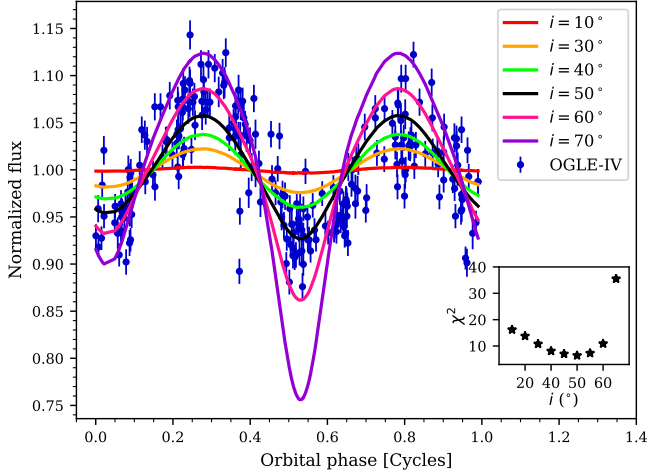


Figure 7. The phase folded OGLE-IV light curve with the synthetic light curves produced with PHOEBE at different inclination angles. *Inset:* Reduced χ^2 values for the OGLE-IV light curve fitted with the synthetic light curves at different inclination angles.

supported by the γ velocity of the He II RV curve being blue-shifted with respect to He I.

4.4 [HP99] 159 as an SSS

It has already been noted that the observed, and steady, L_X can be explained by a mass accretion rate of $\dot{M} \sim 1.5 \times 10^{-7} M_\odot \text{ yr}^{-1}$, but the SSS paradigm requires steady He-burning on the WD surface and that needs a mass-transfer rate significantly ($\sim 5\text{-}10\times$) higher. So, is [HP99] 159 really comparable to other SSS in the Magellanic Clouds and the Milky Way? Firstly, we compare their observed properties in Table 4, where it is clear that while [HP99] 159 is at the faint end of the list, it is actually slightly brighter than CAL87 (as expected given its lower i). So this issue is not unique to [HP99] 159.

This comparison can be taken further by recognising that in the canonical SSS the dominant light source is the accretion disc, and that will be heated by the close-to-Eddington limited SSS emission from the WD. This makes them analogous to their LMXB (low-mass X-ray binary) cousins, where [van Paradijs & McClintock \(1994\)](#) (hereafter vPM94) had shown that there was a correlation between their M_V and a combination of their L_X and P_{orb} (the latter of course links to the size of the accretion disc). That correlation was $M_V = 1.57 - 2.27 \log \Sigma$, where $\Sigma = (L_X/L_{\text{Edd}})^{1/2} (P/1\text{hr})^{2/3}$, and it was used by [van Teeseling et al. \(1997\)](#) to show that a very similar curve fits the SSS as well.

We take the opportunity here to update this relationship by including [HP99] 159 and exploiting the now more accurate galactic distances available from Gaia DR3. The new $M_V - \Sigma$ plot for the SSS in Table 4 is shown in Figure 8, together with a simple straight-line fit (the red line), as well as the original vPM94 black line that fits the steady LMXBs. As they noted (and also [Revnivtsev et al. 2012](#)), since Σ is a flux, then the slope of this line should be -2.5 , and accordingly we show (blue line) the fit with the slope so fixed. This demonstrates an important point. The SSS as a group are clearly displaced above the LMXBs, and so have, for a given value of Σ , an M_V that is 1.5 mags brighter. We believe that this is due to the much larger discs and donors of SSS relative to the LMXBs, essentially doubling the

Table 4. SSS Key Properties

Source	V (range)	$\log L_X$ (erg s^{-1})	P_{orb} (d)	Notes
Magellanic Clouds				
CAL83	16.2–17.1	37.3	1.04	450 d on-off cycle
CAL87	19–21	36.7	0.44	eclipsing
RX J0513.9-6951	17.4	37.8	0.76	170 d on-off cycle
1E 0035.4-7230	20.3	37.3	0.17	short P_{orb}
ASASSN-16oh	16.5–20.5	37.0	5.6	~ 1 yr outburst
[HP99] 159	16	36.8	2.33	this paper
Galactic				
QR And	11.5–12.6	37.1	0.66	$E(B-V)=0.10$
V Sge	10.5–14	36.7	0.51	$E(B-V)=0.33$
MR Vel	17.9	38.0	4.03	$E(B-V)=2.1$

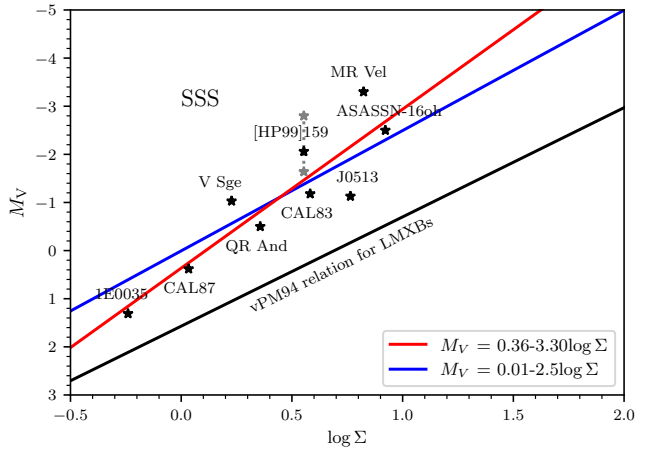


Figure 8. M_V against $\log \Sigma$ for the luminous SSS in the Magellanic Clouds and the Milky Way (adapted from [van Teeseling et al. 1997](#), Fig. 3). The red line is a straight-line fit for the SSS and the blue line is a fit with the slope fixed at -2.5 . The black line is not a fit, but simply the relation for LMXBs ($M_V = 1.57 - 2.27 \log \Sigma$) derived by vPM94 assuming the emission is driven by X-ray irradiation of the disc.

irradiated areas, as is clearly demonstrated by the schematic diagram (Fig. 3) in [Hachisu & Kato \(2003\)](#).

However, [HP99] 159 is different from all other SSS in that it has a He star donor, which should be optically luminous in its own right, contributing significantly to the M_V of -2.8 for [HP99] 159. From [Götberg et al. \(2018\)](#) and [Kato et al. \(2023\)](#) we estimate that a $0.8 M_\odot$ He star will have $M_V = -2.03$, and this leads to $M_V = -2.06$ for the SSS component alone, which is the value we have used in Figure 8 (see also [Kato et al. 2023](#)). The gray star above [HP99] 159 indicates the SSS component $M_V = -1.83$ if the He star has a $M_V = -2.23$ (determined from the 28 yr decay model) and the gray star below [HP99] 159 indicates the SSS component $M_V = -1.64$ if the He star has a $M_V = -2.34$ (determined from the 80 yr decay model). This makes it quite consistent with the other known SSS. We also note that the [Hachisu & Kato \(2003\)](#) interpretation indicates likely considerable mass outflows from the system. Outflows out of the plane of the orbit will show a much lower radial velocity modulation against orbital phase, which could explain our spectroscopic observations.

4.5 Comparison with other He star binaries

We investigated whether [HP99] 159 is comparable to other known systems. In fact, there are a few WD-He star binaries that are of interest as SN Ia candidates, namely KPD 1930+2752 (Geier et al. 2007), V445 Pup (Kato & Hachisu 2003), HD 49798 (Brooks et al. 2017), CD-30° 11223 (Vennes et al. 2012) and PTF1 J2238+7430 (Kupfer et al. 2022). Of particular interest from this group is V445 Pup, which underwent a nova outburst in 2000, and remarkably also showed no hydrogen lines in its spectrum, making it the first He nova (Kato & Hachisu 2003), and hence potentially analogous to [HP99] 159. Interestingly, Schaefer (2025) shows that the WD of V445 Pup appears to be losing mass after each eruption, making it less likely to undergo a SNIa explosion.

However, there were two forms of He star companion considered (see e.g. Woudt et al. 2009 and references therein) for V445 Pup, one a non-degenerate, evolved He star, the other a fully degenerate He WD (also known as AM CVn systems). These latter, double-degenerate binaries, have very short orbital periods (usually ≤ 60 mins). This is significant, as very recently, Schaefer (2025) has proposed an orbital period for V445 Pup of 1.87 d, based on long-term archival (pre-nova) optical photometry. But his resulting folded light curve is very similar in shape and amplitude to that of [HP99] 159 when folded on half the orbital period, and so we suspect that the true period of V445 Pup is actually 3.75 d. More importantly, such a long period automatically rules out the AM CVn scenario, and so V445 Pup is definitely worth comparing more closely with [HP99] 159.

4.6 Binary evolution

From the properties of the expanding nebula surrounding V445 Pup, Woudt et al. (2009) have derived a precise distance of 8.2 ± 0.5 kpc, and estimate an E(B-V) of 0.62 (and hence an $A_V \sim 2.5$). Furthermore, there are strong arguments for a massive WD ($\sim 1.35 M_\odot$) and Kato et al. (2008) indicate that $M_2 > 0.8 M_\odot$, which, combined with $P_{\text{orb}} = 3.75$ d, gives $R_2 = 4.7 R_\odot$. These are very similar parameters to those we have derived for [HP99] 159 in Table 3, and are consistent with what is expected for He star evolution as described in Götberg et al. (2018) and Kato et al. (2023).

Regarding the actual binary system evolution, we note that Podsiadlowski (2010) has modelled binary evolution in the ‘‘supersoft’’ channel of potential SNIa systems. In particular, his Fig. 2 produces, after $\sim 2 \times 10^6$ yrs, a $\sim 1 M_\odot$ WD accreting at $\sim 10^{6-7} M_\odot \text{ yr}^{-1}$ from a donor of $M_2, R_2 = 2.1 M_\odot, 4.6 R_\odot$. This was based on the observed properties of the recurrent nova U Sco, which also bear comparison with [HP99] 159, especially since it was found (Johnston & Kulkarni 1992) to be ‘‘H-deficient’’. Also targeting U Sco, Hachisu et al. (1999) produce a system with a $\sim 1 M_\odot$ WD accreting from a $\sim 2 - 3.6 M_\odot$ companion with a $\sim 0.5 - 5$ d orbital period (see their Fig. 1.F). Of relevance to [HP99] 159 is that the donor has a ‘‘He-rich envelope’’ acquired from the pre-WD in an earlier phase of its evolution.

5 CONCLUSIONS

Our extensive spectroscopic and photometric study of [HP99] 159 has shown that:

- it has remained within ± 0.1 mag of its mean $I \sim 16$ level over the last 14 years, with no indication of decay in the light curve;
- together with the constant blackbody temperature determined by G23, this provides strong evidence that [HP99] 159 is not in the decaying phase of a helium nova event as was suggested by Kato et al.

(2023), and that it should be considered as a comparable member of the group of Magellanic Cloud SSS;

- a PDM period analysis of the OGLE-IV light curve and the phase-resolved spectroscopic results confirm that $P_{\text{orb}} = 2.327$ d;
- we see only helium emission lines in the spectrum, indicating that the donor was likely an (originally) $\sim 4 M_\odot$ He star;
- our He II RV curve yields $\gamma = 273 \pm 1 \text{ km s}^{-1}$ and $K_1 = 9 \pm 1 \text{ km s}^{-1}$ in conflict with our double-peaked orbital light curve regarding the binary i , which we believe to be closer to $i \sim 50^\circ$;
- we propose that substantial mass outflow from the system accounts for the low RV modulation amplitude;
- we propose a donor mass range of $M_2 \sim 1.2 - 2.0 M_\odot$, very similar to the He nova V445 Pup;
- this confirms that [HP99] 159 is indeed the first SSS with an evolved helium donor and therefore a single-degenerate scenario SNIa progenitor;
- we have demonstrated a clear ~ 1.5 mag difference in M_V of SSS systems when compared to the $M_V - \Sigma$ properties of LMXBs.

ACKNOWLEDGEMENTS

Firstly, we thank the anonymous referee for a constructive report that has improved the presentation of our results. Some of the observations reported in this paper were obtained with the Southern African Large Telescope (SALT), under programme 2021-2-LSP-001 (PI: DAHB), the 1.0-m telescope and the 1.9-m telescope located at the Sutherland station of the South African Astronomical Observatory (SAAO). Polish participation in SALT is funded by grant No. MNiSW DIR/WK/2016/07. This paper also used observations made by the Optical Gravitational Lensing Experiment (OGLE). PAC would like to thank Patrick Woudt for useful discussions on V445 Pup, and also acknowledges the Leverhulme Trust for an Emeritus Fellowship. DAHB acknowledges research support from the National Research Foundation. HS acknowledges research support from the Department of Higher Education and Training, RSA. The OGLE project has received funding from the Polish National Science Centre grant OPUS-28 2024/55/B/ST9/00447 to AU.

DATA AVAILABILITY

The data underlying this article will be shared on reasonable request to the corresponding author.

REFERENCES

Alard C., Lupton R. H., 1998, *ApJ*, **503**, 325
 Bowman D. M., Holdsworth D. L., 2019, *A&A*, **629**, A21
 Bramall D. G., et al., 2010, in McLean I. S., Ramsay S. K., Takami H., eds, Society of Photo-Optical Instrumentation Engineers (SPIE) Conference Series Vol. 7735, Ground-based and Airborne Instrumentation for Astronomy III. p. 77354F, doi:10.1117/12.856382
 Bramall D. G., et al., 2012, in McLean I. S., Ramsay S. K., Takami H., eds, Society of Photo-Optical Instrumentation Engineers (SPIE) Conference Series Vol. 8446, Ground-based and Airborne Instrumentation for Astronomy IV. p. 84460A, doi:10.1117/12.925935
 Brooks J., Kupfer T., Bildsten L., 2017, *ApJ*, **847**, 78
 Buckley D. A. H., Swart G. P., Meiring J. G., 2006, in Stepp L. M., ed., Society of Photo-Optical Instrumentation Engineers (SPIE) Conference Series Vol. 6267, Ground-based and Airborne Telescopes. p. 62670Z, doi:10.1117/12.673750

Burdanov A. Y., Krushinsky V. V., Popov A. A., 2014, *Astrophysical Bulletin*, **69**, 368

Coppejans R., et al., 2013, *PASP*, **125**, 976

Crause L. A., et al., 2014, in Ramsay S. K., McLean I. S., Takami H., eds, Society of Photo-Optical Instrumentation Engineers (SPIE) Conference Series Vol. 9147, Ground-based and Airborne Instrumentation for Astronomy V. p. 91476T, doi:10.1117/12.2055635

Crause L. A., et al., 2016, in Ground-based and Airborne Instrumentation for Astronomy VI. p. 990827, doi:10.1117/12.2230818

Crawford S. M., et al., 2010, in Silva D. R., Peck A. B., Soifer B. T., eds, Society of Photo-Optical Instrumentation Engineers (SPIE) Conference Series Vol. 7737, Observatory Operations: Strategies, Processes, and Systems III. p. 773725, doi:10.1117/12.857000

Czesla S., Schröter S., Schneider C. P., Huber K. F., Pfeifer F., Andreasen D. T., Zechmeister M., 2019, PyA: Python astronomy-related packages (ascl:1906.010)

Eggleton P. P., 1983, *ApJ*, **268**, 368

Everett M. E., Howell S. B., 2001, *PASP*, **113**, 1428

Geier S., Nesslinger S., Heber U., Przybilla N., Napiwotzki R., Kudritzki R. P., 2007, *A&A*, **464**, 299

Götberg Y., de Mink S. E., Groh J. H., Kupfer T., Crowther P. A., Zapartas E., Renzo M., 2018, *A&A*, **615**, A78

Greiner J., et al., 2023, *Nature*, **615**, 605

Hachisu I., Kato M., 2003, *ApJ*, **598**, 527

Hachisu I., Kato M., Nomoto K., Umeda H., 1999, *ApJ*, **519**, 314

Johnston H. M., Kulkarni S. R., 1992, *ApJ*, **396**, 267

Kahabka P., van den Heuvel E. P. J., 2006, in Lewin W. H. G., van der Klis M., eds, , Vol. 39, Compact stellar X-ray sources. Cambridge University Press, Cambridge, pp 461–474

Kato M., Hachisu I., 2003, *ApJL*, **598**, L107

Kato M., Hachisu I., Kiyota S., Saio H., 2008, *ApJ*, **684**, 1366

Kato M., Hachisu I., Saio H., 2023, *MNRAS: Letters*, **525**, L56

Kniazev A. Y., Gvaramadze V. V., Berdnikov L. N., 2016, *MNRAS*, **459**, 3068

Kniazev A. Y., Gvaramadze V. V., Berdnikov L. N., 2017, in Balega Y. Y., Kudryavtsev D. O., Romanyuk I. I., Yakunin I. A., eds, Astronomical Society of the Pacific Conference Series Vol. 510, Stars: From Collapse to Collapse. p. 480 (arXiv:1612.00292), doi:10.48550/arXiv.1612.00292

Kupfer T., et al., 2022, *ApJL*, **925**, L12

Massey P., 1997, A User's guide to CCD Reductions with IRAF, Available at http://ircamera.as.arizona.edu/Astr_518/irafguid.pdf, Accessed on 18 March 2019

Mróz P., et al., 2024, *ApJS*, **273**, 4

Podsiadlowski P., 2010, *Astronomische Nachrichten*, **331**, 218

Prša A., et al., 2016, *ApJS*, **227**, 29

Revnivtsev M. G., Zolotukhin I. Y., Meshcheryakov A. V., 2012, *MNRAS*, **421**, 2846

Rucinski S. M., 2001, *AJ*, **122**, 1007

Ruiter A. J., 2020, in Barstow M. A., Kleinman S. J., Provencal J. L., Ferrario L., eds, IAU Symposium Vol. 357, White Dwarfs as Probes of Fundamental Physics: Tracers of Planetary, Stellar and Galactic Evolution. pp 1–15 (arXiv:2001.02947), doi:10.1017/S1743921320000587

Schaefer B. E., 2025, *ApJ*, **980**, 156

Shafter A. W., 1983, *ApJ*, **267**, 222

Smak J. I., Belczynski K., Zola S., 2001, *Acta Astron.*, **51**, 117

Southwell K. A., Livio M., Charles P. A., O'Donoghue D., Sutherland W. J., 1996, *ApJ*, **470**, 1065

Udalski A., Szymanski M., Kaluzny J., Kubiak M., Mateo M., 1992, *Acta Astron.*, **42**, 253

Udalski A., Szymański M. K., Szymański G., 2015, *Acta Astronomica*, **65**, 1

Vennes S., Kawka A., O'Toole S. J., Németh P., Burton D., 2012, *ApJL*, **759**, L25

Wong T. L. S., Schwab J., 2019, *ApJ*, 878, 100

Woudt P. A., Steeghs D., 2005, in Hameury J. M., Lasota J. P., eds, Astronomical Society of the Pacific Conference Series Vol. 330, The Astrophysics of Cataclysmic Variables and Related Objects. p. 451 (arXiv:astro-ph/0409525), doi:10.48550/arXiv.astro-ph/0409525

Woudt P. A., et al., 2009, *ApJ*, **706**, 738

Wozniak P. R., 2000, *Acta Astron.*, **50**, 421

Yoon S. C., Langer N., 2004, *A&A*, **419**, 645

van Paradijs J., McClintock J. E., 1994, *A&A*, **290**, 133

van Teeseling A., Reinsch K., Hessman F. V., Beuermann K., 1997, *A&A*, **323**, L41

This paper has been typeset from a $\text{\TeX}/\text{\LaTeX}$ file prepared by the author.